Applied Catalysis B: Environmental 127 (2012) 351–362

Contents lists available at SciVerse ScienceDirect

Applied Catalysis B: Environmental

journal homepage: www.elsevier.com/locate/apcatb

Pt–Ag/activated carbon catalysts for water denitration in a continuous reactor: Incidence of the metal loading, Pt/Ag atomic ratio and Pt metal precursor

A. Aristizábal[a], S. Contreras[a,*], N.J. Divins[b], J. Llorca[b], F. Medina[a]

[a] Departament d'Enginyeria Quimica, Universitat Rovira i Virgili, Campus Sescelades, Av/Països Catalans 26, 43007 Tarragona, Spain
[b] Institut de Tècniques Energètiques i Centre de Recerca en Nanoenginyeria, Universitat Politècnica de Catalunya, Diagonal 647, 08028 Barcelona, Spain

ARTICLE INFO

Article history:
Received 18 May 2012
Received in revised form 19 July 2012
Accepted 29 August 2012
Available online 8 September 2012

Keywords:
Pt–Ag
Catalytic nitrates reduction
Metal content
Packed bed reactor
Surface metal chemistry

ABSTRACT

Several Pt–Ag catalysts supported on activated carbon powder were tested in the catalytic reduction of nitrates in a continuous flow reactor. The influence of the noble metal precursor ($Pt(NH_3)_4(NO_3)_2$ or H_2PtCl_6), the Pt/Ag atomic ratio (0.3, 1.1 and 1.8) and the metal loading (3% or 1% Pt) were studied. The samples were characterized by XRD, TPR, HRTEM, XPS, H_2-chemisorption and nitrogen physisorption. The results showed that the most important variables affecting the catalytic activity are the noble metal precursor and the metal loading, whereas the Pt/Ag atomic ratio does not affect significantly the catalytic behavior. The use of H_2PtCl_6 instead of $Pt(NH_3)_4(NO_3)_2$ as noble metal precursor leads to more active catalysts. The nitrate conversion is enhanced by the high metal loading (3%).

1. Introduction

The rising nitrate concentration in groundwater [1,2] encourages the scientific community to first improve the technologies for nitrate removal in water, and then to implement these technologies in large-scale facilities to treat water for human consumption [3]. Recent studies in the catalytic reduction of nitrates in water have been focused on the development of selective bimetallic catalysts aimed toward preferential nitrogen formation, which is the major challenge to overcome for the further implementation of this technique [4–6]. In this process, nitrogen selectivity must be strictly near 100% to fulfill the requirements for potable water [7]. Previous studies have shown that the selectivity is extremely dependent on the support material [8,9], the type of metal precursor [6], the bimetallic pair [10,11] and the ratio between the metals in the bimetallic catalysts [10,12,13], among others.

Generally, bimetallic catalysts used for the nitrate reduction in water consist on a metal promoter easily oxidizable and reducible under the reaction conditions (like Cu, Sn, In) and a noble metal able to chemisorb hydrogen (Pd, Pt, Rh) [10,12,14,15], both loaded on a support. It has been demonstrated that both metals, denominated bimetallic pair, crucially determine the catalytic activity and selectivity of this reaction [6,10,11,16]. Most of the studies used a Pd–Cu [6,10,14,17–19] bimetallic pair, and more recently Pd–Sn [16,20,21] and Pd–In [22]; these metals showed the highest selectivity toward nitrogen, which to date is still insufficient considering the strict limitations enforced by the drinking water regulations [23]. However, the use of less studied promoters, like silver (Ag), could be interesting in light of previous studies. $Pd–Ag/Al_2O_3$ bimetallic catalysts showed higher activities and lower ammonium selectivities than Pd–Cu and Pt–Cu catalysts when the correct synthesis protocol was selected [10]. Moreover, $Pd–Ag/Al_2O_3$ showed high nitrogen selectivities, in a range between 66% and 93% [24]. Also, Ag could be an interesting promoter to control microorganisms in water due to its antibacterial action [25], giving another advantage to the catalytic technology over other techniques like biological denitrification.

To the best of our knowledge, few studies in the literature have used Ag as promoter [6,10,16,24,26–30]. All of these studies used semi-batch reactors, but to date there are no literature reports using Ag-based catalysts in continuous systems. Additionally, all these studies used Pd as noble metal, except for Gauthard et al. [10] that reported the activity of $Pt–Ag/Al_2O_3$ catalysts but not the selectivity. Further research using Pt–Ag bimetallic pair would be interesting considering that Pt also showed interesting results in Cu-based catalysts for this reaction [12,31].

Most of the studies have used a 5% content of Pd, however for economic consideration this amount should be minimized. Moreover, Gauthard et al. [10] reported that the activity of Pd–Ag and Pt–Ag catalysts supported on alumina was affected by the Pt/Ag atomic ratio, reporting an optimum value of 1. However, the

* Corresponding author. Tel.: +34 977559680; fax: +34 977559621.
E-mail address: sandra.contreras@urv.cat (S. Contreras).

0926-3373/$ – see front matter © 2012 Elsevier B.V. All rights reserved.
http://dx.doi.org/10.1016/j.apcatb.2012.08.039

incidence of this variable (determinant for the nitrogen formation [6,17,32–35]) in the selectivity achieved by Ag catalysts was not reported.

Moreover, changing the support significantly affects the catalytic behavior in the nitrate reduction in water [8,36–38] and recent studies have shown that activated carbon (AC) gives higher selectivities than alumina in this reaction [8,21,39–42]. However, only Al_2O_3 and CeO_2 were used as support in the studies concerning Ag-based catalysts. The Pt–Ag bimetallic pair supported on AC seems to be an interesting catalytic system and its study might contribute to the understanding and validation of the reaction mechanism of the catalytic reduction of nitrate in water. Additional studies are still needed to optimize the formulation of the Ag-based catalysts and to understand the differences in the nitrogen selectivity due to the promoter [43].

The aim of this work is to study the influence of the Pt/Ag atomic ratio in the activity and selectivity of Pt–Ag supported on AC catalysts in the reduction of nitrate in water in a continuous flow reactor. Moreover, it has been reported in the literature that the metal loading and the metal promoter can affect the metal dispersion and the surface metal chemistry of the metals dispersed on the support [6,37]. Therefore, the AC support was impregnated with 1% or 3% Pt content using different Pt precursors: $Pt(NH_3)_4(NO_3)_2$ or H_2PtCl_6. The fresh and reduced catalysts were characterized by: XRD, TPR, TEM, HRTEM, XPS, nitrogen physisorption and H_2-chemisorption in order to explain the catalytic differences among the catalysts.

2. Experimental

2.1. Support characterization

The physical and chemical characteristics of the support has an important role in the activity and selectivity of AC supported catalysts [8]. The BET surface area, the pore volume and diameter of the AC was determined by nitrogen physisorption. Also, the pH_{PZC} of the AC powder was measured using the pH drift method. A 0.01 M NaCl was prepared and then 20 cm^3 aliquots were placed into 5 beakers. The pH of the aliquots was adjusted between pH 2 and pH 12 by adding HCl or NaOH. Ar was bubbled through the modified solutions at 25 °C to remove dissolved carbon dioxide until the initial pH values were stabilized. A total of 0.12 g of AC was added to each solution. The AC and the solutions were in contact during 24 h under stirring. Afterwards, the final pH was recorded. The graphs of final pH versus initial pH were used to determine the points at which the initial pH was equal to the final pH. This point was taken as the pH_{PZC} of the carbon [44].

2.2. Catalysts characterization

2.2.1. Textural properties

The BET surface area of the catalysts was determined in a physisorption equipment (Micromeritics ASAP 2010 apparatus), from the nitrogen adsorption isotherms at 77 K. Prior to the analysis the samples were degasified 7 h at 120 °C.

2.2.2. H_2 chemisorption

H_2 chemisorption (H_2-chemisorption) analyses were performed in a Micromeritics ASAP 2010 apparatus. The samples were reduced in situ under the same conditions as the catalysts before the analyses (350 °C during 3 h). After reduction, the H_2 on the metal surface was removed with He. The samples were subsequently cooled to 35 °C under the same He stream. The chemisorbed H_2 was analyzed at 35 °C.

2.2.3. Powder X-ray diffraction

Powder X-ray diffraction (XRD) patterns were measured using a Bruker-AXS D8-Discover diffractometer with a parallel incident beam (Gobel mirror) and a vertical θ–θ goniometer, a 0.02° receiving slit and a scintillation counter as a detector. The angular 2θ diffraction range was between 5° and 70°. The data were collected with an angular step of 0.05° at 3 s per step. Cu Kα radiation was obtained from a copper X-ray tube operated at 40 kV and 40 mA. X-ray patterns were compared to X-ray powder references to confirm phase identities using the Joint Committee on Powder Diffraction Standards (JCPDSs, 2006) files. Some of the samples were also reduced at 350 °C during 3 h under H_2 flow (analogous to the catalytic tests) and suspended in ethanol to be analyzed by XRD in order to determine differences due to pretreatment of the catalysts.

2.2.4. High resolution transmission electron microscopy

HRTEM analyses were performed to selected samples with a JEOL 2010F microscope equipped with a field emission gun. The point to point resolution of the instrument was 0.19 nm and the resolution between lines was 0.14 nm. The samples were deposited from ultrasonicated ethanol suspensions over grids with holey-carbon films. Prior to the analysis, samples were reduced at 350 °C during 3 h under H_2 flow (analogous to the catalytic tests).

2.2.5. X-ray photoelectron spectroscopy

X-ray photoelectron spectra (XPS) were recorded at a pressure below 10^{-9} mbar with a SPECS system equipped with an Al anode XR50 source operating at 150 W and a Phoibos MCD-9 detector (pass energy 25 eV). Prior to the analysis, the samples were reduced in situ under 350 °C and atmospheric pressure in a SPECS high pressure cell integrated in the system. Binding energies (accuracy ±0.1 eV) were referred to the adventitious carbon C 1s signal.

2.2.6. Hydrogen temperature programmed reduction

Temperature programmed reduction (H_2-TPR) analyses were performed in a TPD/R/O 1100 (ThermoFinnigan) equipped with a thermal conductivity detector (TCD). About 0.1 g of the sample were placed in a quartz reactor and reduced in a stream of 20 cm^3/min of H_2 (5%, v/v in Ar) at a heating rate of 5 °C/min heated up to 750 °C. The H_2 consumption due to the reduction of the samples was continuously monitored by the TCD. CuO standard calibration curve was used to determine H_2 consumption.

2.3. Catalyst synthesis

For the catalysts preparation, $Pt(NH_3)_4(NO_3)_2$ (Alfa Aeser, CAS 20634-12-2) or H_2PtCl_6 (Johnson Mathew, CAS 98032-39-4) were used as noble metal precursor, and silver nitrate ($AgNO_3$, CAS 7761-88-8, Aldrich) as promoting metal precursor. AC powder (Aldrich, Ref.: 26001-0 Charcoal powder. AC Norit A decolorizing, CAS 64365-11-3) was used as catalysts support.

Pt and Ag monometallic catalysts were impregnated by incipient-wetness technique on AC with an aqueous solution containing the metal precursors. After impregnation the catalysts were dried at 80 °C overnight.

Pt–Ag bimetallic catalysts with different Pt/Ag atomic ratios (1.8, 1.1 and 0.33 atm Pt/atm Ag) and two Pt metal loadings (fixing 3%Pt or 1%Pt in weight basis) were prepared by sequential incipient-impregnation protocol. The Pt/Ag ratio was varied fixing the Pt content in the catalysts. Firstly, the dried support was impregnated with an aqueous solution containing the noble metal precursor ($Pt(NH_3)_4(NO_3)_2$ or H_2PtCl_6) and then dried at 80 °C overnight. Secondly, an aqueous solution of $AgNO_3$ was impregnated and then dried at 80 °C overnight. A total of 12 bimetallic catalysts were synthesized.

2.4. Catalytic tests

The catalysts were tested in the reduction of nitrates in water using H_2 as reducing agent. The reactions were performed at atmospheric conditions (1 atm and 25 °C) in a continuous PBR. The reactor was packed with 1 g of catalyst. The catalysts were reduced at 350 °C under 7 cm^3/min of H_2 for 3 h. Afterwards, 1.2 cm^3/min of a 100 mg/L nitrate solution ($NaNO_3$, Riedhel de Haen) prepared in Milli-Q water were fed to the reactor to start the reaction. H_2 flow was maintained during the entire experiment. The catalytic tests were performed at least twice to check the reproducibility of the results. Each hour a sample of the treated effluent was taken to be analyzed by HPLC.

The catalytic activity of the AC support was studied under the same experimental conditions mentioned for the catalysts. The adsorptive capacity of the support was studied under the same experimental conditions, except that H_2 was not fed when the nitrate flow was fed to the reactor.

Concentrations of nitrate, nitrite and ammonium ions of the aqueous samples were determined by HPLC using a conductivity detector. Nitrate and nitrite concentrations were determined using the anion separation column Shodex IC SI-90 4E (Eluent: 1.7 mM $NaHCO_3$ + 1.8 mM Na_2CO_3) for suppression method. Ammonium concentration was determined using a Shodex IC YK-421 column (Eluent: 5 mM Tartaric Acid + 1 mM Dipicolinic Acid + 1.5 g/L Boric Acid + 0.8 mM Crown Ether).

Ag and Pt concentrations in effluents were analyzed by Inductively Coupled Plasma (ICP) Mass Spectrometry to detect possible leaching. Before the analysis the samples were preserved with concentrated nitric acid (1%, v/v).

The conversion and selectivities at steady state are calculated as:

$$X_{\text{nitrate}} = \frac{(C_{0\,\text{nitrate}} - C_{\text{nitrate}})}{C_{0\,\text{nitrate}}} \times 100 \quad (1)$$

$$S_{\text{nitrite}} = \frac{C_{\text{nitrite}}}{C_{0\,\text{nitrate}} - C_{\text{nitrate}}} \times \frac{62\,\text{g nitrate}}{1\,\text{mol nitrate}} \times \frac{1\,\text{mol nitrite}}{46\,\text{g nitrite}} \times 100 \quad (2)$$

$$S_{\text{ammonium}} = \frac{C_{\text{ammonium}}}{C_{0\,\text{nitrate}} - C_{\text{nitrate}}} \times \frac{62\,\text{g nitrate}}{1\,\text{mol nitrate}} \times \frac{1\,\text{mol ammonium}}{18\,\text{g ammonium}} \times 100 \quad (3)$$

$$S_{\text{nitrogen}} = 100 - S_{\text{nitrite}} - S_{\text{ammonium}} \quad (4)$$

$$\sum S_i = 100 \quad (5)$$

The yields are calculated as:

$$Y_i = \frac{X_{\text{nitrate}}}{100} \times S_i \quad (6)$$

$$\sum Y_i = X_{\text{nitrate}} \quad (7)$$

where X_{nitrate} is the nitrate conversion at steady state (%); S_i the selectivity toward product i at steady state (%); Y_i the yield toward product i at steady state (%) and i is nitrite, nitrogen or ammonium.

C_{nitrate}, C_{nitrite}, C_{ammonium} are the concentrations at steady state of nitrates, nitrites and ammonium respectively, expressed in mg/L. $C_{0\,\text{nitrate}}$ refers to the concentration in the nitrate feed. For the nitrogen selectivity calculation, it is assumed that no other by-products are formed as confirmed in previous studies [45]. Nitrogen production was not monitored.

3. Results and discussion

3.1. Results of support characterization

Carbon materials are considered to be suitable catalytic supports for the reduction of nitrates in water [8]. However, differences in the characteristics of the activated carbon have been reported to affect the catalytic activity [8,46]. Therefore, in order to report the characteristics of the material used as support, the AC was characterized by nitrogen physisorption (Table S1) and pH drift method (see Fig. S1). The AC has a BET area of 651 m^2/g and a pH_{PZC} of 8.8, similar to previous reports [8,47]. Moreover, the AC powder was sieved using a 100 mesh to control particle size. A relatively small particle size of the AC (<100 mesh) was selected in order to minimize mass transfer limitations during the catalytic tests [48].

3.2. Catalysts characterization results

3.2.1. Textural properties

The BET surface areas of the Pt–Ag/AC catalysts are in a range between 402 to 576 m^2/g and 606 to 631 m^2/g, for 3%Pt and 1%Pt content (Table S2), respectively. A decrease in the BET surface area of the samples with respect to the original AC (651 m^2/g) is observed after Pt and Ag impregnation [42,49,50]. This decrease might be caused by the partial blocking of the AC pores that takes place upon impregnation; metal particles may be deposited on the surface of the AC pores decreasing the available surface area [50]. The BET area decreases when metal loading increases; this effect is stronger in $Pt(NH_3)_4(NO_3)_2$ than in H_2PtCl_6 catalysts. Moreover, for the same Pt precursor the BET area decreases when the total metal content increases, i.e. the atomic ratio decreases and/or the metal loading increases.

3.2.2. H_2 chemisorption

Some selected samples were analyzed by H_2-chemisorption in order to compare the accessibility of Pt surface to hydrogen. The results are shown in Table 1.

According to the literature, the H_2 uptake of bimetallic Pt–Ag catalysts is reduced compared to monometallic Pt catalysts after the addition of Ag, which does not chemisorb H_2 at 40 °C [51]. This agrees with the results, showing that a higher Ag addition leads to a decrease in the H_2 uptake in H_2PtCl_6 catalysts (Table 1), indicating that Ag is being partially deposited on the Pt surface (confirmed by XPS) as observed by Epron and co-workers [10]. Moreover, the use of $Pt(NH_3)_4(NO_3)_2$ leads to a higher Pt accessibility and surface area than using H_2PtCl_6 (at atomic ratio 1.8 and 1%Pt content). This shows that fewer Ag is deposited on the Pt surface when $Pt(NH_3)_4(NO_3)_2$ is used (later confirmed by XPS data).

3.2.3. Powder X-ray diffraction

The XRD profiles of the AC support and the as-synthesized monometallic catalysts are shown in Fig. 1. The AC support (Fig. 1A) presents diffraction peaks at 2θ = 26.6°, 20.9°, 45.8° and 42.5° 39.3°, 50.1° and 59.9,° assigned to graphite (JCPDS 00-026-1077) and

Table 1
H_2-chemisorption results of Pt–Ag/AC catalysts.

Catalyst	Pt precursor	Pt/Ag	Ratio	Pt surface area	
				m^2/g sample	m^2/g Pt
1%Pt–0.3%Ag/AC	$Pt(NH_3)_4(NO_3)_2$	1.8	9.9	0.25	24.6
1%Pt–0.3%Ag/AC	H_2PtCl_6	1.8	6.2	0.15	15.4
1%Pt–0.5%Ag/AC	H_2PtCl_6	1.1	3.1	0.08	7.8

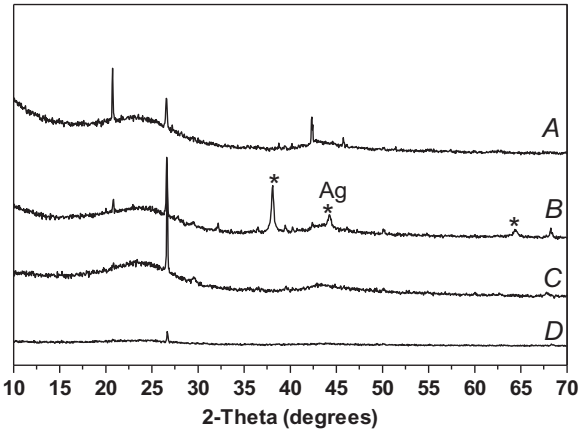

Fig. 1. XRD patterns of: (A) AC, (B) 1.5%Ag/AC, (C) 3%Pt/AC ($Pt(NH_3)_4(NO_3)_2$) and (D) 3%Pt/AC (H_2PtCl_6) monometallic catalysts.

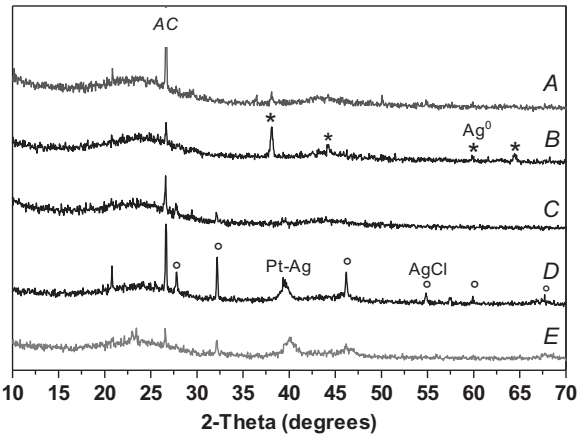

Fig. 2. XRD patterns of bimetallic catalysts with atomic ratio 1.1: (A) 1%Pt–0.5%Ag/AC ($Pt(NH_3)_4(NO_3)_2$), (B) 3%Pt–1.5%Ag/AC ($Pt(NH_3)_4(NO_3)_2$), (C) 1%Pt–0.5%Ag/AC (H_2PtCl_6), (D) 3%Pt–1.5%Ag/AC (H_2PtCl_6) and (E) reduced 3%Pt–1.5%Ag/AC (H_2PtCl_6).

SiO_2 (JCPDS 00-033-1161), as the reflections are overlapped. These reflections are observed in all samples and their intensities varies due to the heterogeneity of the bulk composition of the support, well known characteristic of ACs [52].

3.2.3.1. Monometalic catalysts. Respect monometallic catalysts, 1.5%Ag/AC sample (Fig. 1B) shows well-defined diffraction lines at $2\theta = 38.2^\circ$, 44.2° and 64.3° (JCPDS 04-0783 and 01-1167) characteristic of the (1 1 1) planes of Ag^0 crystallites, as previously observed by Gang et al. [53]. The Ag^0 formation is probably due to the photoreduction of $AgNO_3$. The presence of weak reflections at $2\theta = 32.1^\circ$, 33.8°, 37.2°, $38.2^\circ$and 50.1° suggest the formation of Ag_2O (JCPDS 01-072-2108).

Pt monometallic catalysts (Fig. 1C and D) do not show additional reflections to AC, as previously reported by Antolini et al. [54], suggesting a high metal dispersion and the formation of particles smaller than the detection limit (1–2 nm) of the XRD technique [55]. The same behavior is observed no matter the Pt precursor and metal loading (3% or 1% Pt).

3.2.3.2. Bimetallic catalysts. Fig. 2 presents the XRD patterns of the Pt–Ag bimetallic catalysts with an atomic ratio of 1.1, as representative samples. Samples with Pt/Ag atomic ratios 1.8 and 0.3 present similar diffraction lines according to the metal loading and Pt precursor. Bimetallic catalysts present additional reflections to the ones assigned to the AC support.

Fig. 2A and B shows representative XRD patterns of fresh bimetallic catalysts prepared from $Pt(NH_3)_4(NO_3)_2$ as Pt precursor. Well-defined peaks of metallic silver at $2\theta = 38.1^\circ$, 43.9°, 44.4°, 59° and 64.2° (JCPDS 01-1167 and 02-1098) are observed in all samples. The intensity of the peaks increases with the Ag content in the catalysts. However, these peaks are not observed in samples with a 1.8 atomic ratio (not shown) possibly due to the low Ag content (less than 1%). No reflections associated to metallic Pt ($2\theta = 39.7^\circ$, 46.3° and 67.2°, JCPDS 04-0802) or Pt–Ag solid solution particles are detected, possibly due to the formation of small particles not detectable by XRD [55].

Fig. 2C and D shows representative XRD samples prepared from H_2PtCl_6 as Pt precursor. The samples present AgCl reflections at $2\theta = 27.8^\circ, 32.2^\circ, 46.2^\circ, 54.8^\circ, 57.4^\circ, 67.4^\circ$ (JCPDS 031-1238), and the intensity of these peaks increases with the Ag content. Differences in the XRD patterns among the samples suggest that the particle size of the AgCl entities increases with metal loading, as reported by Yoshinaga et al. [37]. Reflections attributed to Pt–Ag solid solution are observed in all cases. These peaks are less crystalline in samples containing 1% Pt probably due to a smaller metal particle size. Peaks related to Pt^0, Ag^0 and silver oxides are not observed but their presence is not discarded.

Additionally, samples with a Pt/Ag atomic ratio 1.1 were reduced under H_2 flow in the catalytic system and then analyzed by XRD. These samples presented the same XRD reflections observed for fresh samples. $Pt(NH_3)_4(NO_3)_2$ samples (not shown) show Ag^0 reflections; while reduced samples prepared from H_2PtCl_6 (Fig. 2E) show reflections attributed to Pt–Ag solid solution and AgCl, but in this case the peaks are less intense probably due to the smaller

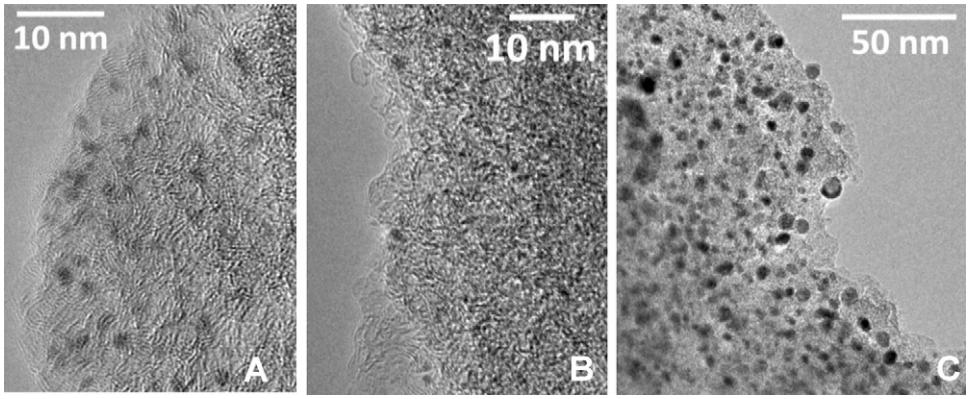

Fig. 3. Low-magnification TEM image of bimetallic samples after reduction: (A) 1%Pt–0.5%Ag/AC (H_2PtCl_6), (B) 3%Pt–1.5%Ag/AC (H_2PtCl_6) and (C) 3%Pt–1.5%Ag/AC ($Pt(NH_3)_4(NO_3)_2$).

metal particle size (confirmed by TEM). Reflections due to Ag^0 or Pt^0 phases are not observed, maybe due to the small particle size and high dispersion.

3.2.4. High resolution transmission electron microscopy

Some samples were reduced (350 °C, 2 h under H_2 flow) and then analyzed by HRTEM to determine the particle size and to confirm the Pt–Ag solid solution formation detected by XRD.

Fig. 3 shows a representative low-magnification image of each analyzed sample. In these cases, individual metal particles with spherical shape are well-distributed over the carbon support and no particle aggregates are encountered in these samples.

Table 2 presents the mean particle diameter of the reduced samples with a Pt/Ag atomic ratio of 1.1. Given the high electron contrast between metal particles and the carbon support, the direct measurement of particle size is accurate.

The mean particle size diameter of reduced samples is significantly smaller than in the fresh samples (see TEM analyses of fresh samples, Table S3). It seems that the reduction pre-treatment decreases the mean particle size, and this is probably due to the reduction of the metal precursors and AgCl, and to a re-dispersion of Ag^0 and Pt–Ag phases detected by XRD of fresh samples.

Moreover, the Pt precursor salt seems to play an important role in the final particle size of the metals in the support. It appears that samples prepared from H_2PtCl_6 contain metal particles smaller than those prepared from $Pt(NH_3)_4(NO_3)_2$ as a precursor. The higher dispersion of the metallic phase in H_2PtCl_6 catalysts could be due to the formation of mobile $[Pt_VO_xCl_y]$s species, which are reported to enhance the Pt distribution on the catalytic support and the support's acidity due to chlorine [56]. Moreover, the use of the tetraammine complexes has been reported to achieve lower Pt dispersions [42,57,58], which is attributed to the intermediate formation of a mobile species, probably $[Pt(NH_3)_2H_2]$, leading to easy agglomeration. To obtain higher dispersions using Pt tetraammine complexes, it is necessary a thermal decomposition under He prior to complete reduction. This effect is not observed in the fresh Pt–Ag catalysts (see TEM results in supplementary information) probably because the formation of the mobile species that affect the dispersion requires temperature when using the tetraammine complex. The spontaneous reduction of the metal precursors upon contacting the carbon surface or their hydrolysis on the surface (forming easily reducible oxide or hydroxide species on the support surface) might lead to the formation of massive particles of a metallic or oxidic phase, respectively, leading to a low dispersion of the Pt in the fresh catalysts. However, the same processes could give rise to numerous metallic or easily reducible particles capable of serving as metal nuclei upon reduction [42].

Furthermore, it seems that increasing the metal loading increases the metal particle size, in accordance with the XRD and TEM results of fresh samples.

Concerning the formation of solid solutions, detailed lattice-fringe images have been recorded for the selected reduced samples and the results are presented in Fig. 4.

In Fig. 4A and B, detailed microstructure of particle labeled "a" (in the figures) and their corresponding Fourier transform (FT) images are shown. The position of spots at 0.232 and 0.202 nm indicate that the particles are oriented along the [0 1 1] crystallographic axis. Taking into account that both metallic Pt and Ag exhibit face-centered cubic structure, these spots correspond to the (1 1 1) and (2 0 0) crystallographic planes with a cell parameter of 0.402–0.404 nm. The cell parameter for pure Pt is 0.3923 nm and for Ag is 0.4086 nm. Considering a linear relationship between lattice parameter and composition (Vegard's law), the value of

Table 2
Mean metal particle diameter of reduced Pt–Ag/AC catalysts.

Reduced sample	Pt/Ag atomic ratio	Pt precursor	d_{Mean} (nm)
1%Pt–0.5%Ag/AC	1.1	H_2PtCl_6	1.2
3%Pt–1.5%Ag/AC	1.1	H_2PtCl_6	1.7
3%Pt–1.5%Ag/AC	1.1	$Pt(NH_3)_4(NO_3)_2$	4.1

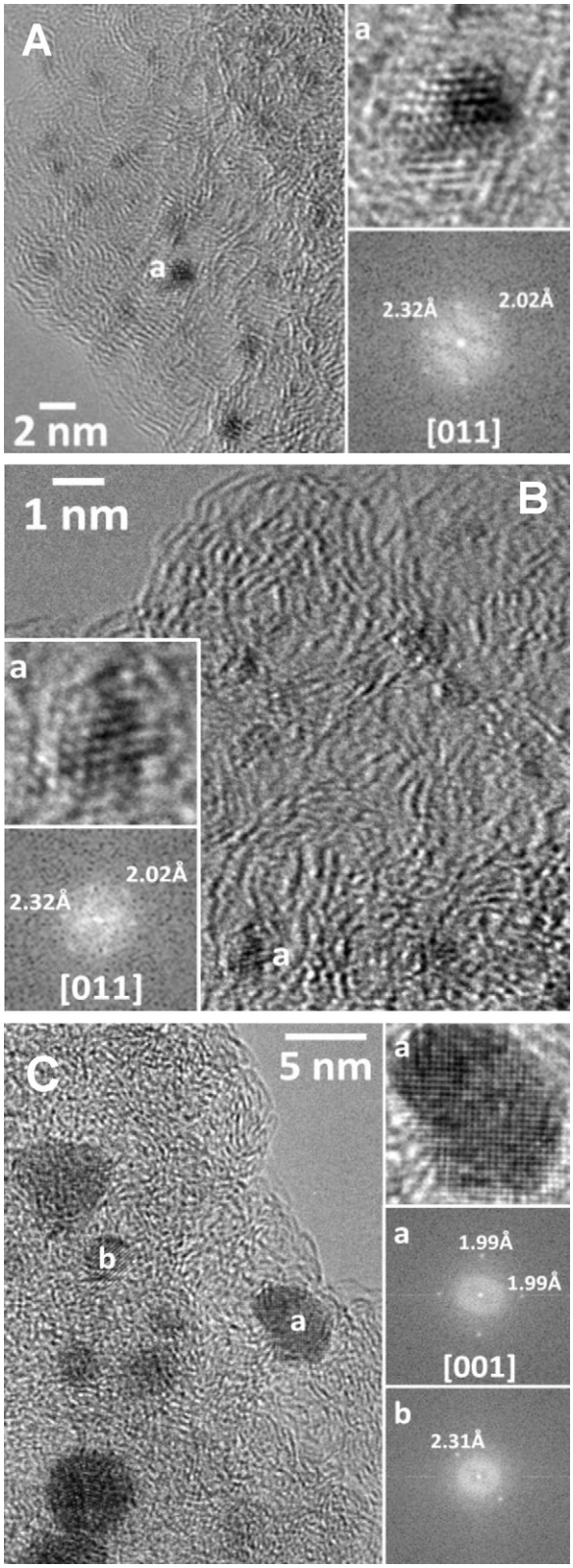

Fig. 4. HRTEM image of bimetallic samples after reduction: (A) 1%Pt–0.5%Ag/AC (H_2PtCl_6), (B) 3%Pt–1.5%Ag/AC (H_2PtCl_6) and (C) 3%Pt–1.5%Ag/AC ($Pt(NH_3)_4(NO_3)_2$).

Table 3
Surface Pt/Ag atomic ratios and binding energies of Pt 4f calculated by XPS.

Catalysts	Pt precursor	Pt/Ag atomic ratio		Binding energy (eV)	
		Theoretical	XPS	Pt $4f_{7/2}$	Pt $4f_{5/2}$
1%Pt–0.3%Ag/AC	H_2PtCl_6	1.8	0.64	71.1	74.6
1%Pt–0.5%Ag/AC	H_2PtCl_6	1.1	0.42	71.4	74.9
3%Pt–1.5%Ag/AC	H_2PtCl_6	1.1	0.71	71.2	74.6
3%Pt–1.5%Ag/AC	$Pt(NH_3)_4(NO_3)_2$	1.1	0.80	71.5	75.0

0.402–0.404 nm indicates the formation of a Pt–Ag solid solution [59]. Fig. 4C exhibits the lattice fringes in a catalyst prepared from $Pt(NH_3)_4(NO_3)_2$. This catalyst contains larger metal particles. The spots at 0.199 nm correspond to the (2 0 0) crystallographic plane with a lattice parameter of 0.398 nm, which are indicative of a Pt–Ag solid solution as well. Particle "b" exhibits (1 1 1) spots at 0.231 nm, which correspond to a solid solution particle with a lattice parameter of 0.4 nm. These results agree with the XRD patterns of H_2PtCl_6 reduced samples. Pt^0 or Ag^0 particles are not observed, but their presence is not discarded.

Therefore, it can be concluded that in these reduced samples Pt–Ag solid solution particles occur and the particle size is the main difference among them.

3.2.5. X-ray photoelectron spectroscopy

Taking into account the differences in the catalytic surface introduced by the reduction pre-treatment, selected samples were in situ reduced under H_2 flow and then analyzed by XPS to determine the valence state of the active metals in the support and the Pt/Ag surface atomic ratio. The Pt 4f spectra of the in situ reduced Pt–Ag/AC catalysts, show a doublet with a low energy band (Pt $4f_{7/2}$) and a high energy band (Pt $4f_{5/2}$) around 71.3 eV and 74.6 eV (Table 3). The shift of the Pt 4f band positions to lower energy values with respect to Pt/AC (found to be 71.6 and 74.8 eV, as in [55,60]) suggest electron transfer from Ag to Pt, which could be related to Pt–Ag solid solution formation [60] in catalysts prepared from H_2PtCl_6, as observed by HRTEM. At 350 °C the Pt on the surface is totally reduced as reported in [61,62] and in accordance with the H_2-TPR results. The Ag 3d spectra shows a doublet composed by a low energy peak (Ag $3d_{5/2}$) and a high energy peak (Ag $3d_{3/2}$) at 368.1 eV and 374.2 eV for samples prepared from H_2PtCl_6 (the same values were obtained for Ag/AC monometallic catalyst). A shift to higher values in each band of 0.1 eV is observed for the samples prepared from $Pt(NH_3)_4(NO_3)_2$ (368.2 and 374.2 eV). These peaks are indicative of metallic Ag [63], as confirmed by XRD of the reduced samples.

Table 3 presents the Pt/Ag atomic ratio calculated by XPS and the corresponding BE of Pt 4f.

It is observed that the composition on the surface is different from the bulk composition (Table 3), i.e. the Pt/Ag surface atomic ratios are lower than the theoretical values. This suggests a silver enrichment on the surface also observed by the H_2-chemisorption results. This difference may be related to the synthesis protocol, since Pt is firstly deposited and then silver in a second impregnation step. The depth of XPS analysis is between 2 and 10 nm, and in the reduced samples the particles observed by HRTEM are between 1.2 and 4.1 nm (Table 2), which means that roughly the entire particle is analyzed, if located at the outer shell of the support. Considering this, more Pt-rich particles may be located in the pores and then not analyzed by XPS; whereas larger particles, rich in Ag (more difficult to disperse), may be located outside the pores, more at the outer shell of the support, and then, analyzed by XPS. Besides this, the silver enrichment can also be due to the lower surface energy of silver with respect to Pt, which causes the migration of silver to the surface [60].

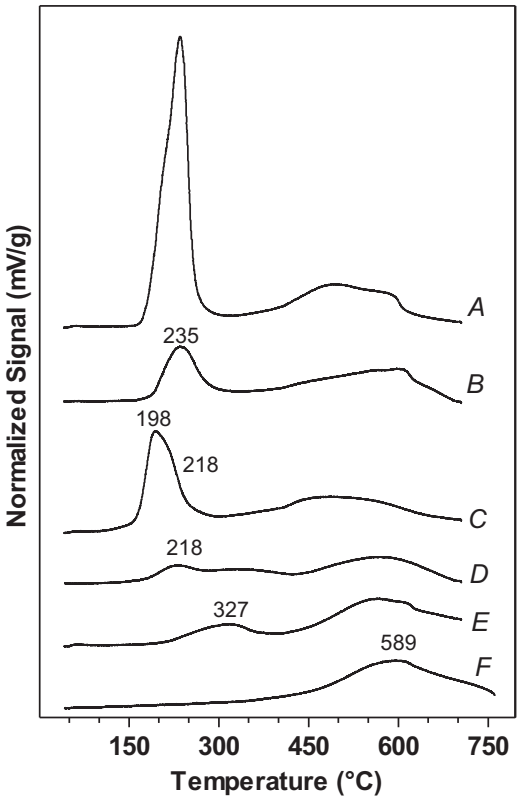

Fig. 5. H_2-TPR profiles of monometallic catalysts: (A) 3%Pt/AC ($Pt(NH_3)_4(NO_3)_2$), (B) 1%Pt/AC ($Pt(NH_3)_4(NO_3)_2$), (C) 3%Pt/AC (H_2PtCl_6), (D) 1%Pt/AC (H_2PtCl_6), (E) 1.5%Ag/AC ($AgNO_3$) and (F) AC.

Moreover, it seems that when H_2PtCl_6 is used, the decrease on the Pt/Ag ratios is more pronounced than in the $Pt(NH_3)_4(NO_3)_2$ sample, suggesting that the Ag enrichment of the Pt surface is higher when H_2PtCl_6 is used, also confirmed by H_2-chemisorption results. Also, considering the same Pt/Ag ratio, when metal loading increases the Ag enrichment decreases.

3.2.6. H_2 temperature programmed reduction

The samples were analyzed by H_2-TPR to determine the H_2 consumptions and the differences in the reducibility of the samples.

3.2.6.1. Monometallic catalysts. The H_2-TPR profiles of the monometallic catalysts and AC are presented in Fig. 5.

The AC support (Fig. 5F) presents a reduction peak around 589 °C, which may be attributed to the gasification of the AC and the decomposition of oxygen surface groups by temperature to produce CO_2 and CO [25,61,64].

After metal impregnation, new peaks at a relatively low temperature appear in the H_2-TPR of monometallic catalysts (Fig. 5) respect to the AC profile (Fig. 5F). In all Pt monometallic catalysts occurs a shift to lower reduction temperatures of the peak assigned to the reduction of the AC support. This shift is related to the enhancement of the carbon gasification by H_2 activation and spillover on the Pt metallic sites [61]. This effect is not observed in 1.5%Ag/AC catalysts (Fig. 5E) because Ag^0 does not chemisorbs H_2 as confirmed by H_2-chemisorption.

Table 4 shows the theoretical and actual H_2 consumptions of monometallic catalysts. Actual H_2 consumptions were calculated by integration of the low temperature peak in the H_2-TPR profiles (peaks that appear after metal impregnation of the support).

H_2PtCl_6 monometallic catalysts present peaks at lower reduction temperature than $Pt(NH_3)_4(NO_3)_2$. Pt/AC catalysts prepared

Table 4
Theoretical and actual H_2 consumptions of monometallic catalysts.

Catalysts	Precursor	$H_{2,TPR}$ (mmol/g)	$H_{2,Theoretical}$[a] (mmol/g)
3%Pt/AC	$Pt(NH_3)_4(NO_3)_2$	1.53	1.38
1%Pt/AC	$Pt(NH_3)_4(NO_3)_2$	0.48	0.46
3%Pt/AC	H_2PtCl_6	0.73	0.31
1%Pt/AC	H_2PtCl_6	0.25	0.10
1.5%Ag/AC	$AgNO_3$	0.21	0.63

[a] $H_{2,Theoretical}$ is the value calculated assuming a decomposition of the salt precursors to HCl, NH_3 and H_2O [65,66].

Table 5
H_2 consumption calculated from the H_2-TPR profiles of fresh bimetallic catalysts.

Catalysts	Pt/AgAtomic ratio	$H_{2,TPR}$ (mmol/g)	
		$Pt(NH_3)_4(NO_3)_2$	H_2PtCl_6
1%Pt–1.7%Ag/AC	0.3	0.81	0.53
1%Pt–0.5%Ag/AC	1.1	0.96	0.55
1%Pt–0.3%Ag/AC	1.8	0.57	0.31
3%Pt–5.0%Ag/AC	0.3	1.85	0.95
3%Pt–1.5%Ag/AC	1.1	1.62	0.99
3%Pt–0.9%Ag/AC	1.8	1.42	0.92

from $Pt(NH_3)_4(NO_3)_2$ (Fig. 5A and B) present a main peak at 235 °C. In the case of Pt/AC catalysts prepared from H_2PtCl_6, a peak at 218 °C is observed for metal loading 1%Pt, while for 3%Pt a peak at 198 °C with a shoulder at 218 °C are observed [66,67].

The hydrogen consumption in Pt/AC catalysts is mainly attributed to the reduction of the Pt precursors. However, the actual H_2 consumptions ($H_{2,TPR}$) are 8% and 50% superior than the expected values ($H_{2,Theoretical}$) for $Pt(NH_3)_4(NO_3)_2$ and H_2PtCl_6 catalysts, respectively (Table 4). These differences indicate that the consumed H_2 is not only invested in the reduction of deposited Pt salts to a zero valence state. The additional H_2 consumption could be related to the decomposition of the functional groups of the support, as previously reported in Pt/AC monometallic catalysts [42,61,62,68]. During and after the reduction of Pt, H_2 is chemisorbed on the Pt metal particles formed and is then spilt over the surface of the support, reducing the functional groups of the AC support in competition with the reduction of the remaining reducible Pt species [42]. This second effect is stronger in H_2PtCl_6 catalysts, may be due to the higher metal dispersion observed in HRTEM of reduced samples.

Therefore, taking into account that H_2-TPR profile of AC support do not show H_2 consumption at reduction temperatures under 450 °C, it is concluded that the dissociation of molecular hydrogen only occurs on Pt-containing catalysts, but not on the support alone as reported by Román-Martínez et al. [68].

Ag/AC catalyst (Fig. 5E) presents a relative low temperature peak around 327 °C, attributed to the reduction of the precursor salt and Ag_2O (confirmed by XRD) [25]. The actual H_2 consumption of this peak is 65% lower than the theoretical value, suggesting that the precursor is partially reduced to the metallic state during the impregnation, as confirmed by XRD. In this case the reduction of the surface functional groups of AC at low reduction temperatures occurs because Ag^0 does not chemisorb H_2, as confirmed by H_2-chemisorption.

In summary, an important H_2 consumption at relatively low temperatures is observed in monometallic catalysts due to the reduction of the precursor salts. Additionally, in Pt monometallic catalysts this process overlaps with the reduction of the surface functional groups of the AC support by hydrogen spillover. Pt and Ag are completely reduced to zero valent state after a treatment with H_2 at 350 °C.

3.2.6.2. Bimetallic catalysts. The H_2-TPR profiles of the bimetallic catalysts prepared from $Pt(NH_3)_4(NO_3)_2$ and H_2PtCl_6 are presented in Figs. 6 and 7, respectively. Table 5 shows the H_2 consumptions for the bimetallic catalysts.

$Pt(NH_3)_4(NO_3)_2$: The H_2-TPR profiles of Pt–Ag bimetallic catalysts using $Pt(NH_3)_4(NO_3)_2$ as precursor (Fig. 6) present a main reduction peak around $T_{max} \sim 235$ °C, additionally to the peak assigned to AC (Fig. 5F), as observed by Gauthard et al. [10]. This

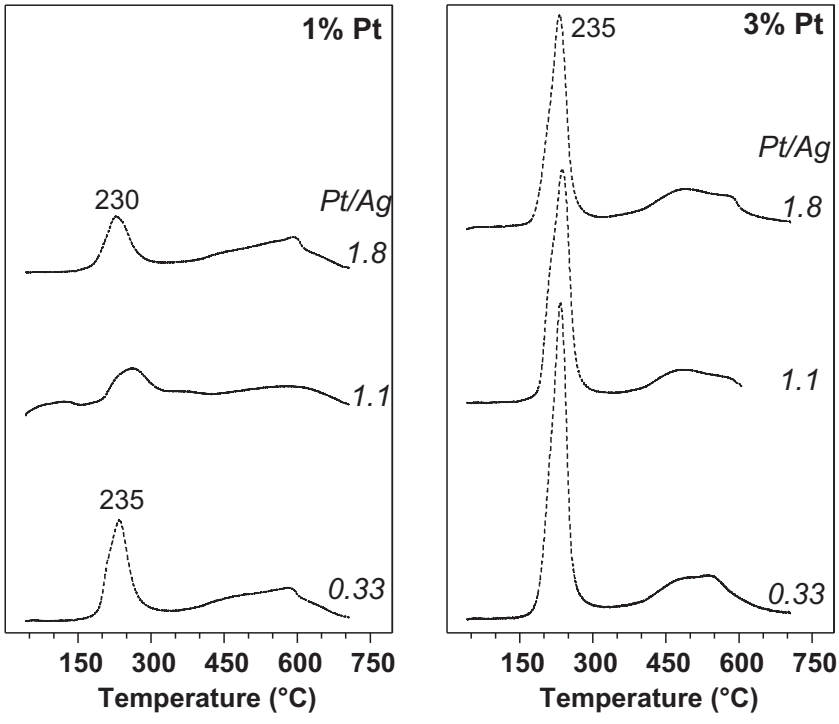

Fig. 6. H_2-TPR profiles of Pt–Ag/AC catalysts prepared from $Pt(NH_3)_4(NO_3)_2$ as Pt precursor at different metal loadings and Pt/Ag ratios.

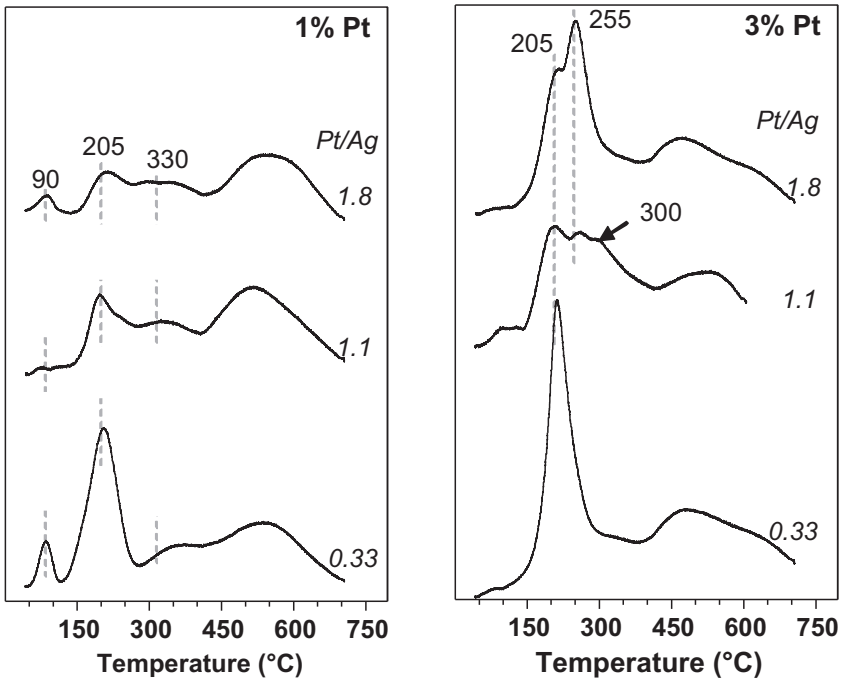

Fig. 7. H_2-TPR profiles of bimetallic catalysts impregnated using H_2PtCl_6 as precursor, at different metal loadings and Pt/Ag atomic ratio.

narrow and symmetrical peak indicates a uniform composition of the reducible species. This H_2 consumption is mainly attributed to the reduction of the Pt precursor, due to the similarity to the peak observed in the corresponding Pt/AC catalysts (Fig. 5A and B). Nevertheless, the actual H_2 consumption of bimetallic samples is higher than the reported for monometallic samples, and it is inferred that it is also related to the reduction of Ag species in close contact with Pt, which agrees with the formation of Pt–Ag solid solution particles after reduction pre-treatment confirmed by HRTEM and XPS. However, this last contribution to H_2 consumption should be lower than in Ag/AC due to the partial reduction of the Ag species during impregnation (confirmed by the Ag^0 reflection in XRD), to the absence of reflection of Pt–Ag solid solution in XRD, and to the absence of reduction peaks around 327 °C in fresh samples (Fig. 6), as observed in Ag/AC (Fig. 5E). Considering this, the H_2 consumption due to the reduction of the surface functional groups of AC by spillover (as described for Pt monometallic catalysts) might also occur, but in lesser extent compared to monometallic samples due to the Ag presence that does not chemisorb H_2, as confirmed by H_2-chemisorption.

As an exception, sample 1%Pt–0.5%Ag (Pt/Ag ratio 1.1) shows an additional reduction peak at relatively lower temperatures, which might be due to the highly dispersed Pt species.

For these catalysts, when the Pt/Ag ratio increases a slight decrease of the reduction temperature is observed in all samples with the same Pt content, as Pt is nobler than Ag. The intensity of the peak increases when the total metal loading increases (i.e. the Pt/Ag decreases and the Pt loading increases) because more reducible species are present, confirmed by H_2 consumption.

H_2PtCl_6: Fig. 7 shows the H_2-TPR profiles of bimetallic catalysts prepared from H_2PtCl_6. At high reduction temperatures a peak due to the reduction of AC appears, as described previously. And at relatively lower temperatures different maxima are identified within a range between 50 and 400 °C, contrary to Pt/AC monometallic catalysts (Fig. 5C and D) that only presents one main peak. The complexity of these profiles suggests a wide range of compositions of the metallic phases formed in the catalysts that strongly varies with the Pt/Ag atomic ratio, contrary to catalysts prepared from $Pt(NH_3)_4(NO_3)_2$.

The first peak around $T_{max} \sim 90$ °C observed in all samples prepared from H_2PtCl_6, may be related to the reduction of highly dispersed Pt-containing phases or to Pt–Ag solid solution with smaller particle size. The second peak observed around $T_{max} \sim 205$ °C, is probably related to the formation of larger Pt–Ag solid solution particles detected by XRD of fresh catalysts. These peaks are strongly affected by the Pt/Ag ratio, and their intensity increases with the Ag content.

The peaks at higher reduction temperatures, in a range of 240–400 °C, may be mainly due to the reduction of AgCl particles (detected by XRD) or $AgNO_3$ probably in contact with Pt and to the decomposition of functional groups of the AC promoted by hydrogen spillover of Pt, as described for Pt monometallic catalysts [68]. These peaks are shifted to lower reduction temperature compared to the Ag monometallic catalysts. This large region decreases in intensity while the Pt/Ag ratio decreases, probably because there is more formation of AgCl species in contact with Pt.

In conclusion, for the same Pt metal loading and Pt/Ag ratio, higher H_2 consumptions are obtained in catalysts prepared from $Pt(NH_3)_4(NO_3)_2$ than H_2PtCl_6, as observed in Pt monometallic catalysts. Ag-containing phases are more easily reduced when $Pt(NH_3)_4(NO_3)_2$ precursor is used instead of H_2PtCl_6 in bimetallic catalysts, probably due to the non-formation of AgCl. Moreover, the reduction of the active phase occurs at higher temperatures in H_2PtCl_6 catalysts, indicating a stronger metal-support interaction in these samples. As for monometallic catalysts, the H_2 consumption is also due to the hydrogen spillover at relatively low temperature in Pt-containing samples, but the effect is more complex due to the Ag addition.

A temperature of 350 °C is selected to reduce the catalysts to ensure a complete reduction to the metallic phase.

3.3. Adsorption capacity and catalytic activity of the support

The adsorption capacity and the catalytic activity of the AC powder were studied (analogous to the catalytic tests) in order to analyze the incidence of the support in the reaction.

The adsorption or catalytic removal of nitrates by the support is negligible (Fig. S3). No nitrite and ammonium formation or

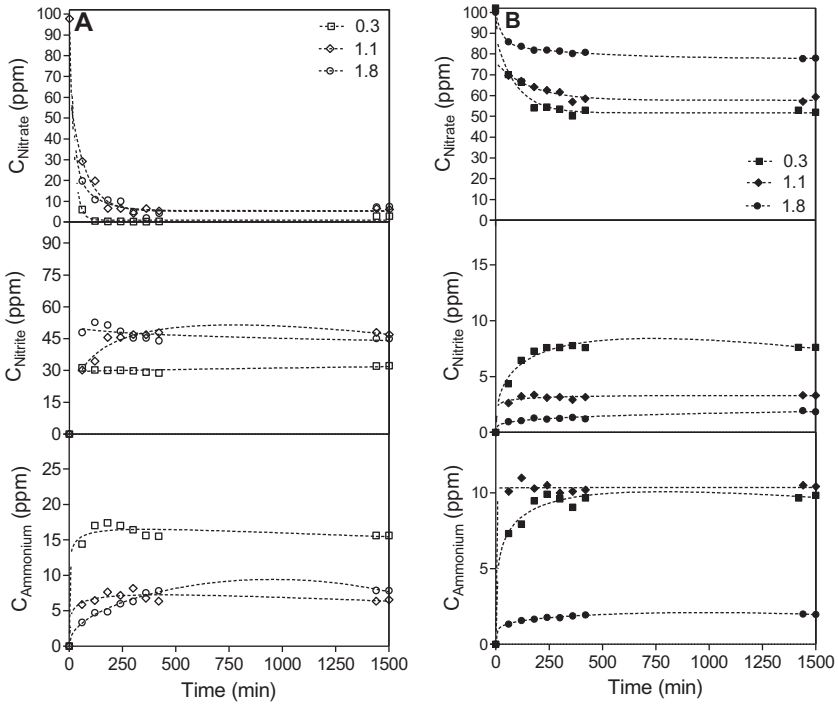

Fig. 8. Nitrate, nitrite and ammonium concentration profiles in time in a continuous reactor with bimetallic catalysts containing 3% Pt and prepared using: (A) H_2PtCl_6 and (B) $Pt(NH_3)_4(NO_3)_2$ as Pt precursor.

desorption are detected. As a conclusion, the presence of a metallic active phase on the surface of the AC support is necessary to remove nitrates.

3.4. Catalytic activity

The catalytic activity of the monometallic catalysts was also studied in the nitrate reduction (results not shown). 1% Ag, 1% Pt (H_2PtCl_6) and 1% Pt ($Pt(NH_3)_4(NO_3)_2$) monometallic catalysts supported on AC are practically inactive for the nitrate reduction as observed by Soares et al. [11]. Therefore, a bimetallic pair is needed to increase the degradation rate of nitrates.

Fig. 8 shows the nitrate, nitrite and ammonium concentration profiles as a function of time for the bimetallic catalysts containing 3% Pt. Similar profiles are observed for catalysts containing 1% Pt. It is observed that catalysts are stable in time, and no Ag or Pt leaching were detected in the effluents by ICP. In all cases, the nitrite and ammonium concentration in steady state surpassed the European maximum admissible concentrations in potable water (0.5 and 0.3 ppm, respectively) [7]. Therefore, it is necessary to improve these results for further large scale application. The high nitrite concentration detected agrees with the results of Gauthard et al. [10]. They observed low activity of silver to reduce nitrites using Ag-based catalysts.

3.4.1. Variation of the nitrate conversion

The nitrate conversions and selectivities achieved by the Pt–Ag/AC bimetallic catalysts in steady state are presented in Table 6.

From Table 6, it is clearly established that the most important variable affecting the nitrate conversion is the Pt precursor. The use of H_2PtCl_6 strongly enhances the conversion compared to employing $Pt(NH_3)_4(NO_3)_2$. This is related to the differences in the metal particle size and/or to the type of bimetallic sites formed with each precursor. Smaller metal particles are obtained using H_2PtCl_6 than $Pt(NH_3)_4(NO_3)_2$ in the reduced samples (HRTEM), leading to a higher metallic surface area which are the active sites for the reaction [23]. These smaller particles could explain the higher conversion. Besides, the formation of AgCl confirmed by XRD of H_2PtCl_6 bimetallic catalysts, seems to cause the deposition of silver in close contact with Pt, which is claimed to enhance the catalytic activity [10].

The second variable affecting the nitrate conversion is the metal loading. When the metal loading increases, the conversion increases for both Pt precursors as observed before [13,37]. This conversion increase is due to the formation of more active sites to reduce nitrates due to a higher metal content. Moreover, the difference in the metal particle size introduced by the higher metal loading seems to induce structure-sensitivity effects that affect

Table 6
Conversion and selectivities of Pt–Ag/AC catalysts at steady state.

Metal loading	$Pt(NH_3)_4(NO_3)_2$				H_2PtCl_6			
	$X_{nitrate}$	$S_{nitrite}$	$S_{ammonium}$	$S_{nitrogen}$	$X_{nitrate}$	$S_{nitrite}$	$S_{ammonium}$	$S_{nitrogen}$
1%Pt–1.7%Ag/AC	6	23.6	35.2	41.3	78	87.2	2.8	10.1
1%Pt–0.5%Ag/AC	13	33.2	36.3	30.6	78	76.1	23.6	0.3
1%Pt–0.3%Ag/AC	12	29.3	25.8	44.9	77	78.2	19.2	2.6
3%Pt–5.0%Ag/AC	49	21.2	68.0	10.8	99	40.8	54.6	4.6
3%Pt–1.5%Ag/AC	43	10.1	80.5	9.4	99	40.1	56.3	3.6
3%Pt–0.9%Ag/AC	21	9.8	32.7	57.5	92	61.9	26.2	11.9

conversion [37]. Also, it seems that counter effects occur at the same time when the metal loading increases. Firstly, the number of metallic active sites increases, evidenced by the increase of the H_2 consumption, resulting in a higher nitrate conversion. Secondly, the increase of the metal particle size diminishes the active surface area, which affects adversely the nitrate conversion afore mentioned. Considering the conversion enhancement due to the increase of the metal loading it can be established that the former effect is stronger.

Additionally, two catalysts with a lower metal loading (0.3%Pt–0.5%Ag/AC, results not shown) were tested at the same reaction conditions. These catalysts were not active even using H_2PtCl_6 as precursor. Concerning the Pt metal loading, 3% Pt is recommended to enhance the nitrate conversion.

The effect of the Pt/Ag atomic ratio on the nitrate conversion is weaker than the other studied variables. The effect of Pt/Ag atomic ratio at low metal loading (1%Pt) is negligible on conversion, whereas at high metal loading (3%Pt) the tendency slightly changes and the nitrate conversion decreases for an atomic ratio of 1.8 for both precursors. This decrease could be explained due to the lower Ag content probably forming less active sites for nitrate reduction. This behavior is in agreement with the results obtained for monometallic catalysts and with the literature, where it is well established that a second metal promoter (like Ag) is necessary to form the active sites to reduce nitrates [23]. Also, this decrease in conversion could be related to a higher metal particle size observed in samples with a ratio of 1.8 (see Supplementary information). This effect is not clearly observed in catalysts with 1%Pt content because the differences in the metal particle size at low metal loading are not significant to be reflected in the catalytic activity. The best atomic ratio to maximize conversion while minimizing the metal content is 1.1. These results agree with the results of Gauthard et al. [10], that reported an optimal atomic ratio of 1 atom Pt/atom Ag for Pt–Ag/Al_2O_3 catalysts.

In conclusion, the best combination to enhance nitrate conversion is to use H_2PtCl_6 as metal precursor and 1.1 Pt/Ag ratio. A Pt metal loading of 3% is recommended, however if economic considerations are taken into account 1%Pt loading for catalysts prepared from H_2PtCl_6 is also acceptable in terms of conversion.

3.4.2. Selectivities

The selectivities are strict constrains in the catalytic reduction of nitrates; the acceptable values are limited by the EU maximum admissible concentrations of nitrates, nitrites and ammonium in potable water (50, 0.5 and 0.3 ppm, respectively [7]).

Table 6 evidences differences in the selectivies of the Pt–Ag/AC catalysts due to the metal loading, Pt/Ag atomic ratio, Pt precursor. Also conversion level is determinant to compare selectivities especially in continuous systems, as previously reported for this reaction [9,45,69]. However, independently of the nitrate conversion, that is significantly different among catalysts, low nitrogen selectivities are obtained in all cases and further work is needed to optimize these values.

3.4.3. Yields

Considering the effect of the conversion level in the selectivities, the products yields at steady state (Eq. (3)) were calculated to compare the results at the same reaction conditions, the results are shown in Table 7. Yields take into account the conversion level and it is more appropriate to compare yields than selectivities when differences in conversions are found.

3.4.3.1. Nitrite. The nitrite yields are strongly affected by the Pt precursor; higher values are obtained using H_2PtCl_6 than $Pt(NH_3)_4(NO_3)_2$. It is well established that the nitrite reduction occurs mainly on the noble monometallic sites [17,33]. Therefore, it is expected that a higher Pt/Ag surface ratio and a higher H_2-chemisorption in $Pt(NH_3)_4(NO_3)_2$ catalysts lead to higher nitrite reduction rate, observed as a lower nitrite selectivity and yield. This agrees with Gauthard et al. [10] who observed that the nitrite reduction activity decreases by the addition of silver to a noble monometallic catalysts. They attributed this behavior to a low activity of silver to reduce nitrites. Besides, the results agree with the study of Horold et al. [6] that reported higher nitrite removal activities when using tetra-amino palladium hydroxide, instead of palladium chloride, in alumina impregnated catalysts. They attributed this behavior to the better adsorption of the cationic tetra-amino complex compared to the anionic tetrachloro-complex. Furthermore, HRTEM analyses of reduced samples suggest that H_2PtCl_6 samples have smaller metal particle size than those of $Pt(NH_3)_4(NO_3)_2$. This smaller size could explain the differences in the nitrite yield by a structure sensitive reaction as previously suggested by Yoshinaga et al. [37].

The nitrite yield is also affected by the metal loading and the atomic ratio, however the effects are different according to the Pt precursor. For H_2PtCl_6 catalysts, the nitrite yield decreases when the metal loading increases, agreeing with the proposed mechanism where nitrite is reduced mainly on Pt monometallic sites [17,33]. With a higher Pt loading a major content of these sites is more probable, as observed experimentally by the increase of the surface Pt/Ag ratio and H_2 consumption. This effect decreases when the atomic ratio increases, at 1.8 Pt atoms/Ag atom the yield remains practically unaffected evidencing an interaction between the metal loading and the atomic ratio. Moreover, the nitrite yield is minimized at Pt/Ag ratio of 1.1 for H_2PtCl_6 catalysts, close to the value described as optimum for Pd–Cu catalysts in the literature.

In the case of $Pt(NH_3)_4(NO_3)_2$ catalysts the nitrite yield remains practically constant around 5%. For this precursor, the yield is not significantly affected by the atomic ratio or the metal loading, except for a Pt/Ag ratio of 0.3, which reported a higher nitrite yield (10%) at high metal loading.

In conclusion, to minimize the nitrite yield it is necessary to use $Pt(NH_3)_4(NO_3)_2$ as Pt precursor and to fix a Pt/Ag atomic ratio of 1.1 with a high metal loading (3%Pt). The data evidenced complex interactions among the Pt precursor, the atomic ratio and the metal loading.

Table 7
Yields of Pt–Ag/AC catalysts at steady state.

Metal loading	Pt/Ag ratio	$Pt(NH_3)_4(NO_3)_2$			H_2PtCl_6		
		$Y_{nitrite}$	$Y_{ammonium}$	$Y_{nitrogen}$	$Y_{nitrite}$	$Y_{ammonium}$	$Y_{nitrogen}$
1%Pt–1.7%Ag/AC	0.3	1.4	2.1	2.5	68.0	2.2	7.9
1%Pt–0.5%Ag/AC	1.1	4.3	4.7	4.0	59.4	18.4	0.2
1%Pt–0.3%Ag/AC	1.8	3.5	3.1	5.4	60.2	14.8	2.0
3%Pt–5.0%Ag/AC	0.3	10.4	33.3	5.3	40.4	54.1	4.6
3%Pt–1.5%Ag/AC	1.1	4.3	34.6	4.0	39.7	55.7	3.6
3%Pt–0.9%Ag/AC	1.8	2.1	6.9	12.1	56.9	24.1	10.9

Table 8
Catalytic results at iso-conversion for Pt–Ag/AC catalysts.

Catalysts	Pt/Ag Atomic ratio	Pt precursor	$X_{nitrates} \approx 45\%$		
			$S_{nitrite}$ (%)	$S_{ammonium}$ (%)	$S_{nitrogen}$ (%)
3%Pt–5.0%Ag/AC	0.3	H_2PtCl_6	32.4	26.8	40.6
		$Pt(NH_3)_4(NO_3)_2$	21.2	68.0	10.8
3%Pt–1.5%Ag/AC	1.1	H_2PtCl_6	30.8	43.0	26.2
		$Pt(NH_3)_4(NO_3)_2$	10.1	80.5	9.4
3%Pt–0.9%Ag/AC	1.8	H_2PtCl_6	53.8	13.7	32.4
		$Pt(NH_3)_4(NO_3)_2$	[a]	[a]	[a]

[a] It is not possible to obtain 45% conversion due to physical constrains of the reaction system.

3.4.3.2. Ammonium. The ammonium yield strongly increases when the Pt metal loading increases from 1 to 3%. The increase in the ammonium yield might be due to the formation of more active sites, which reduce nitrites to ammonium. The metal loading is the most significant variable affecting the ammonium production; these findings agree with those observed by Horold et al. [6].

Considering the same metal loading, the ammonium yield is enhanced when using H_2PtCl_6 rather than $Pt(NH_3)_4(NO_3)_2$. Concerning the Pt/Ag atomic ratio, a maximum yield is obtained at Pt/Ag ratio of 1.1 considering the same Pt salt and metal loading. The ammonium yield decreases with the atomic ratio as follows: 1.1 > 1.8 > 0.3 at low metal loadings (1%Pt), whereas the tendency is 1.1 > 0.3 > 1.8 at high metal loadings (3%Pt).

The differences in the ammonium yield can be explained by differences in the metal particles size and the metallic phases formed on the catalysts surface. Moreover, Yoshinaga et al. [37] stated that if the Cu particles are deposited on the edge or corner sites of Pd in Pd–Cu/AC catalysts, these sites with strong hydrogenation capacity that enhances ammonium production will become inactive. Thus, the selectivity to N_2 would be enhanced by the addition of Cu. However, in the case of Ag-based catalysts, Gauthard et al. [10] reported that the deposition of silver is made randomly on all type of Pt sites, thus increasing the ammonium selectivity.

3.4.3.3. Nitrogen. Pt–Ag/AC catalysts achieved low nitrogen yields (<15%) and significant differences among the catalysts are not observed, except for the increase in the nitrogen yield in catalysts 3%Pt–0.9%Ag/AC with Pt/Ag ratio of 1.8. The nitrogen yield requires improvement for further large scale application of this catalytic system.

3.4.4. Selectivity at iso-conversion

In view of the differences in conversion level among the catalysts, which affect the analyses of the effect of the variables in the selectivity, iso-conversion experiments were carried out. Catalysts with high metal loading (3%Pt) were tested again in the reaction, but this time the retention time of the liquid flow in each experiment was varied to obtain a nitrate conversion of 45%. The retention time was varied by changing the catalyst weight and/or the nitrate flow. This time the effect of the metal loading in the selectivities at iso-conversion in the nitrate reduction in water was not studied. The catalytic results at iso-conversion are presented in Table 8.

3.4.4.1. Nitrite. The nitrite selectivity at iso-conversion is higher when using H_2PtCl_6 than $Pt(NH_3)_4(NO_3)_2$, following the same tendency described for the nitrite yield. This higher nitrite selectivity could be related to the same reasons aforementioned for nitrite yield. Additionally, in iso-conversion experiments the higher nitrite selectivity is also due to the lower retention time of the liquid flow required to decrease conversion in H_2PtCl_6 catalysts. A lower retention time avoid the contact of nitrites with the active sites on the catalysts decreasing the probability to be reduced respect $Pt(NH_3)_4(NO_3)_2$ catalysts, at this conversion level.

It is not possible to determine the effect of the Pt/Ag atomic ratio in the nitrite yield at iso-conversion for $Pt(NH_3)_4(NO_3)_2$ catalysts, because a conversion of 45% was not reached in all the samples due to physical constrains of the reaction system.

3.4.4.2. Ammonium. The ammonium selectivity at iso-conversion is higher in $Pt(NH_3)_4(NO_3)_2$ catalysts than in H_2PtCl_6, contrary to the ammonium yield at different conversion levels. This discrepancy can be attributed to changes in the reaction rates with conversion level. The maximum ammonium selectivity is obtained at ratio 1.1 as aforementioned.

3.4.4.3. Nitrogen. The nitrogen selectivity at iso-conversion is strongly influenced by the Pt precursor. H_2PtCl_6 catalysts achieved higher nitrogen selectivities than $Pt(NH_3)_4(NO_3)_2$. This variation in selectivities might be due to differences in the active sites compositions [45], metal particle size, and/or retention time. Further studies are needed in order to clarify the type of active sites formed in these type of catalysts.

4. Conclusions

The Pt precursor and the metal loading are the most important variables affecting the catalytic behavior of Pt–Ag/AC catalysts for the reduction of nitrates in water, due to the modification of the active sites architecture. The effect of the atomic ratio is of less importance in the range studied for this system. The studied variables affect in different ways the conversion and selectivity, making the methodical optimization of this process a complex procedure.

Higher nitrate conversion and nitrogen selectivity are obtained using H_2PtCl_6 than $Pt(NH_3)_4(NO_3)_2$ as metal precursor. These results might be related to the presence of chlorine, which induces changes in the particle size and Pt–Ag surface metal chemistry after reduction. When H_2PtCl_6 is used, a closer interaction between the metals may be induced and AgCl phase is formed. The importance of the precursors is clear. Therefore, it is important to consider the precursor when comparing different bimetallic pairs or noble metals. Besides, to maximize the conversion a ratio of 1.1 and 3%Pt content are recommended, however these conditions also enhance the ammonium yield.

Pt–Ag/AC catalysts demonstrated to be active and stable to reduce nitrates in water. Nevertheless, nitrites and ammonium concentrations in the effluent need to be diminished in all cases to fulfill the maximum admissible concentrations of potable water.

The Pt–Ag pair is a complex system, which can contribute to increase the understanding of the influence of the surface metal chemistry in the catalytic reduction of nitrates in water. As a result, further experiments are being performed to establish the nature of the differences due to the Pt precursor and the synthesis protocol in Pt–Ag based catalysts.

Acknowledgements

The authors are thankful for the financial support given by Universitat Rovira i Virgili, Spanish Ministry of Science and Innovation (Ramon y Cajal Program funding S.C. and project CTM2008-02453), Fondo Social Europeo and AGAUR (Project 2008ITT-CTP-00111, FI scholarship and ICREA ACADEMIA award funding J.Ll. and F.M.).

Appendix A. Supplementary data

Supplementary data associated with this article can be found, in the online version, at http://dx.doi.org/10.1016/j.apcatb.2012.08.039.

References

[1] R.f.t.C.t.t.C.a.t.E. Parliament, On Implementation of Council Directive 91/676/EEC Concerning the Protection of Waters Against Pollution Caused by Nitrates from Agricultural Sources Based on Member State Reports for the Period 2004–2007, European Commission, Brussels, 2010, p. SEC(2010) 2118.
[2] U.S.G.S. U.S. Department of the Interior, Elevated Nitrogen and Phosphorus Still Widespread in Much of the Nation's Streams and Groundwater, 2010.
[3] N. Barrabés, J. Sá, Applied Catalysis B: Environmental 104 (2011) 1–5.
[4] Y.-X. Chen, Y. Zhang, G.-H. Chen, Water Research 37 (2003) 2489–2495.
[5] A. Pintar, Catalysis Today 77 (2003) 451–465.
[6] S. Horold, K.D. Vorlop, T. Tacke, M. Sell, Catalysis Today 17 (1993) 21–30.
[7] European Communities (Drinking Water) (No. 2), Regulations 2007. Statutory Instruments, http://www.attorneygeneral.ie/esi/2007/esi_num.html#251-300
[8] O.S.G.P. Soares, J.J.M. Órfão, M.F.R. Pereira, Catalysis Letters 139 (2010) 97–104.
[9] A.E. Palomares, C. Franch, A. Corma, Catalysis Today 172 (2011) 90–94.
[10] F. Gauthard, F. Epron, J. Barbier, Journal of Catalysis 220 (2003) 182–191.
[11] O. Soares, J.J.M. Orfao, M.F.R. Pereira, Catalysis Letters 126 (2008) 253–260.
[12] N. Barrabés, J. Just, A. Dafinov, F. Medina, J.L.G. Fierro, J.E. Sueiras, P. Salagre, Y. Cesteros, Applied Catalysis B: Environmental 62 (2006) 77–85.
[13] O.S.G.P. Soares, J.J.M. Órfão, M.F.R. Pereira, Applied Catalysis B: Environmental 91 (2009) 441–448.
[14] J. Sá, H. Vinek, Applied Catalysis B: Environmental 57 (2005) 247–256.
[15] S. Horold, T. Tacke, K.-D. Vorlop, Environmental Technology 14 (1993) 931–939.
[16] A. Devadas, S. Vasudevan, F. Epron, Journal of Hazardous Materials 185 (2011) 1412–1417.
[17] U. Prüsse, K.-D. Vorlop, Journal of Molecular Catalysis A: Chemical 173 (2001) 313–328.
[18] A. Pintar, J. Batista, J. Levec, T. Kajiuchi, Applied Catalysis B: Environmental 11 (1996) 81–98.
[19] Y. Wang, J. Qu, H. Liu, C. Hu, Catalysis Today 126 (2007) 476–482.
[20] I. Dodouche, D.P. Barbosa, M.d.C. Rangel, F. Epron, Applied Catalysis B: Environmental 93 (2009) 50–55.
[21] A. Garron, K. Lazar, F. Epron, Applied Catalysis B: Environmental 59 (2005) 57–69.
[22] I. Witonska, S. Karski, N. Krawczyk, Polish Journal of Chemistry 82 (2008) 171–178.
[23] F. Deganello, L.F. Liotta, A. Macaluso, A.M. Venezia, G. Deganello, Applied Catalysis B: Environmental 24 (2000) 265–273.
[24] I. Witonska, S. Karski, J. Goluchowska, Reaction Kinetics and Catalysis Letters 90 (2007) 107–115.
[25] V.S. Kumar, B.M. Nagaraja, V. Shashikala, A.H. Padmasri, S.S. Madhavendra, B.D. Raju, K.S.R. Rao, Journal of Molecular Catalysis A: Chemical 223 (2004) 313–319.
[26] S. Horold, T. Tacke, K.D. Vorlop, Environmental Technology 14 (1993) 931–939.
[27] K.D. Vorlop, U. Prusse, in: R.A.v.S.e.F.J.J.G. Janssesn (Ed.), Catalytic Science Series, Imperial College Press, London, 1999, p. 369.
[28] S. Karski, Chemical and Environmental Research 15 (2006) 123–132.
[29] U. Prusse, S. Horold, K.D. Vorlop, Chemie Ingenieur Technik 69 (1997) 93–97.
[30] I. Witonska, M. Frajtak, N. Krawczyk, A. Krolak, S. Karski, Przemysl Chemiczny 87 (2008) 941–946.
[31] O. Salomé, J. a. J.M. Órfão, M.R. Pereira, Catalysis Letters 126 (2008) 253–260.
[32] W. Gao, N. Guan, J. Chen, X. Guan, R. Jin, H. Zeng, Z. Liu, F. Zhang, Applied Catalysis B: Environmental 46 (2003) 341–351.
[33] U. Prusse, M. Hahnlein, J. Daum, K.-D. Vorlop, Catalysis Today 55 (2000) 79–90.
[34] O.M. Ilinitch, L.V. Nosova, V.V. Gorodetskii, V.P. Ivanov, S.N. Trukhan, E.N. Gribov, S.V. Bogdanov, F.P. Cuperus, Journal of Molecular Catalysis A: Chemical 158 (2000) 237–249.
[35] Y. Wang, Y. Sakamoto, Y. Kamiya, Applied Catalysis B: Environmental 361 (2009) 123–129.
[36] N. Barrabés, J. Sá, Applied Catalysis B: Environmental 104 (2011) 1–5.
[37] Y. Yoshinaga, T. Akita, I. Mikami, T. Okuhara, Journal of Catalysis 207 (2002) 37–45.
[38] Y. Wang, J. Qu, H. Liu, R. Wu, Chinese Science Bulletin 51 (2006) 1431–1438.
[39] A.E. Palomares, J.G. Prato, F. Márquez, A. Corma, Applied Catalysis B: Environmental 41 (2003) 3–13.
[40] A.E. Palomares, J.G. Prato, F. Rey, A. Corma, Journal of Catalysis 221 (2004) 62–66.
[41] O.S.G.P. Soares, J.J.M. Órfão, M.F.R. Pereira, Desalination 279 (2011) 367–374.
[42] M. Gurrath, T. Kuretzky, H.P. Boehm, L.B. Okhlopkova, A.S. Lisitsyn, V.A. Likholobov, Carbon 38 (2000) 1241–1255.
[43] O.S.G.P. Soares, J.J.M. ÃrfÃ£o, M.F.R. Pereira, Applied Catalysis B: Environmental 91 (2009) 441–448.
[44] B. Xiao, K.M. Thomas, Langmuir 21 (2005) 3892–3902.
[45] A. Aristizábal, S. Contreras, N. Barrabés, J. Llorca, D. Tichit, F. Medina, Applied Catalysis B: Environmental 110 (2011) 58–70.
[46] N. Krawczyk, S. Karski, I. Witońska, Reaction Kinetics, Mechanisms and Catalysis 103 (2011) 311–323.
[47] A. Cabiac, G. Delahay, R. Durand, P. Trens, B. Coq, D. Plée, Carbon 45 (2007) 3–10.
[48] A.J. Lecloux, Catalysis Today 53 (1999) 23–34.
[49] N. Barrabés, A. Dafinov, F. Medina, J.E. Sueiras, Catalysis Today 149 (2010) 341–347.
[50] S.E. Samra, E.A. El Sharkawy, A.M. Youssef, Colloids and Surfaces A: Physicochemical and Engineering Aspects 163 (2000) 199–208.
[51] M.T. Schaal, A.C. Pickerell, C.T. Williams, J.R. Monnier, Journal of Catalysis 254 (2008) 131–143.
[52] A. Dandekar, R.T.K. Baker, M.A. Vannice, Carbon 36 (1998) 1821–1831.
[53] L. Gang, B.G. Anderson, J. van Grondelle, R.A. van Santen, Applied Catalysis B: Environmental 40 (2003) 101–110.
[54] E. Antolini, F. Cardellini, E. Giacometti, G. Squadrito, Journal of Materials and Science 37 (2002) 133–139.
[55] Y.-Y. Feng, G.-R. Zhang, J.-H. Ma, G. Liu, B.-Q. Xu, Physical Chemistry Chemical Physics 13 (2011) 3863–3872.
[56] G.J. Antos, A.M. Aitani, Catalytic Naphtha Reforming, Marcel Dekker, 2004.
[57] F. Rodríguez-Reinoso, I. Rodríguez-Ramos, C. Moreno-Castilla, A. Guerrero-Ruiz, J.D. López-González, Journal of Catalysis 99 (1986) 171–183.
[58] M.C. Román-Martínez, D. Cazorla-Amorós, A. Linares-Solano, C.S.-M.n. De Lecea, H. Yamashita, M. Anpo, Carbon 33 (1995) 3–13.
[59] Z. Peng, H. Yang, Journal of Solid State Chemistry 181 (2008) 1546–1551.
[60] J.B. Xu, T.S. Zhao, Z.X. Liang, The Journal of Physical Chemistry C 112 (2008) 17362–17367.
[61] A.Y. Stakheev, O.P. Tkachenko, G.I. Kapustin, N.S. Telegina, G.N. Baeva, T.R. Brueva, K.V. Klementiev, W. Grunert, L.M. Kustov, Russian Chemical Bulletin 53 (2004) 528–537.
[62] S.R. de Miguel, J.I. Vilella, E.L. Jablonski, O.A. Scelza, C. Salinas-Martinez de Lecea, A. Linares-Solano, Applied Catalysis A: General 232 (2002) 237–246.
[63] A.M. Venezia, Catalysis Today 77 (2003) 359–370.
[64] A. Guerrero-Ruiz, P. Badenes, I. RodrIguez-Ramos, Applied Catalysis A: General 173 (1998) 313–321.
[65] M.K. Oudenhuijzen, P.J. Kooyman, B. Tappel, J.A. van Bokhoven, D.C. Koningsberger, Journal of Catalysis 205 (2002) 135–146.
[66] M.A. Fraga, E. Jordão, M.J. Mendes, M.M.A. Freitas, J.L. Faria, J.L. Figueiredo, Journal of Catalysis 209 (2002) 355–364.
[67] G.C. Torres, E.L. Jablonski, G.T. Baronetti, A.A. Castro, S.R. de Miguel, O.A. Scelza, M.D. Blanco, M.A. Pena Jiménez, J.L.G. Fierro, Applied Catalysis A: General 161 (1997) 213–226.
[68] M.C. Román-Martínez, D. Cazorla-Amorós, A. Linares-Solano, C.S.-M. de Lecea, Carbon 31 (1993) 895–902.
[69] A. Aristizábal, N. Barrabés, S. Contreras, M. Kolafa, D. Tichit, F. Medina, J. Sueiras, Physics Procedia 8 (2010) 44–48.